Radiation Physics and Chemistry 203 (2023) 110606

Contents lists available at ScienceDirect

Radiation Physics and Chemistry

journal homepage: www.elsevier.com/locate/radphyschem

Determination of WER and WET equivalence estimators for proton beams in the therapeutic energy range using MCNP6.1 and TOPAS codes

A.L. Burin *, I.S.L. Branco, H. Yoriyaz

Nuclear and Energy Research Institute, University of São Paulo, Avenue Professor Lineu Prestes, 2242, CEP, 05508000, São Paulo, São Paulo, Brazil

ARTICLE INFO

Keywords:
Proton range
WER
WET
Proton therapy
Monte Carlo simulation

ABSTRACT

To use the dosimetric advantages that proton therapy provides, the exact knowledge of the range and its associated parameters of the beam is essential. Since the human body is composed of several tissues whose composition and density differ from water it is important to relate the range in water to the range in those tissues. Those range associated parameters are the Water Equivalent Ratio (WER) and Water Equivalent Thickness (WET). This work presents the Range, WER and WET values obtained from the simulations using the Monte Carlo codes MCNP6.1 and TOPAS for several tissue-equivalent materials, which are materials that reproduce the radiation behavior of the human tissues in a phantom. Simulations have been done in the therapeutic proton energy range from 70 to 225 MeV. Therefore, the main objective of this work is to provide and contribute to the improvement of dose calculation in proton therapy, more specifically in the calculation of WER and WET in tissue equivalent medium. The results showed good agreement between codes, presenting only small differences less than 1.9% in the cortical bone, but they did not affect the dose calculation in the therapeutic range used in this study.

1. Introduction

Proton therapy is an increasingly relevant form of radiotherapy. Despite the high cost to build a proton treatment center, the possibility of reducing the total dose compared to photons, saving critical structures, while higher and better-conformed doses are delivered to the tumor volume, fully justifies the use of this type of treatment beam. Although it is an already technologically mature modality, there are still many open problems in this field that must be investigated. Accurate knowledge of the range of a proton beam when penetrating the patient's body or other materials is essential and can be defined in terms of the water equivalent thickness - WET (Zhang and Newhauser, 2009). Basically, this parameter depends on the proton energy and material density and composition.

Proton beam dosimetry is usually evaluated in water to represent the patient in calculating the beam range and measuring the absorbed dose. The range that was measured for water is used to calculate the WER and WET which in turn will be used as tissue equivalence estimators (Bagheri et al., 2019; Safigholi and Song, 2018).

Bagheri et al. (2019), determined the water equivalent ratio, WER, for some dosimetric materials like paraffin, polymethyl methacrylate and polyetyrene. One of their conclusions is that polyethylene and paraffin are the most similar to water in terms of dose results. Safigholi and Song (2018) also calculated WER for several materials using various Monte Carlo (MC) codes using proton monoenergetic energies ranging from 10 to 500 MeV. They found good agreement among the results obtained from different MC codes and observed that WER values are greater for higher density materials (higher than water) and decrease rapidly for materials density lower than water in the range of energy of 10–50 MeV. For the range of energy between 100 and 500 MeV the WER values are approximately constant for all materials. Akbari et al. (2014) calculated WER for several dosimetric materials using FLUKA (Ferrari et al., 2005) and SRIM (Ziegler, J.F., Biersack, J.P., Ziegler, 2008) for different monoenergetic proton energies. The calculations were done in a cylindrical phantom determining the dose in cylindrical slice detectors to plot depth dose curves from where WER values were obtained. Very good agreement has been reported between the two codes.

In research for new dosimetric materials, commercial plastic materials characteristics have been analyzed by Lourenço et al. (2017) experimentally and using FLUKA (Ferrari et al., 2005) and Geant4 (Agostinelli et al., 2003) MC codes in low (60 MeV) and high (226 MeV) proton energy beams. They concluded that the plastic-to-water

* Corresponding author.
E-mail addresses: anaburin@usp.br, analauraburin24@gmail.com (A.L. Burin).

https://doi.org/10.1016/j.radphyschem.2022.110606
Received 26 January 2022; Received in revised form 19 September 2022; Accepted 18 October 2022
Available online 24 October 2022
0969-806X/

conversion factors are small, (1% from unity) showing no preference regarding the type of water-equivalent plastic.

WET is also a parameter that can be related to the tomography of patient planning through the calibrated HU (Hounsfied Unit). It can be used in conjunction with CBCT (Cone Beam CT) for the detection of changes in organs and setup errors (Wang et al., 2016). During the treatment, considerable variations have been observed in WET, which have to be taken into account showing to be useful for analysis in adaptive proton therapy. Similar work has been done by Matney et al. (2016), where they investigated the use of WET to quantify the effects of respiratory motion during proton therapy. WET variation was calculated between exhale and inhale phases. This work showed the use of WET to identify cases where the respiratory motions impact on the calculated dose. WET was also used as complementary clinical indicators and to support decision-making process in case of anatomic changes during the treatment (Veiga et al., 2016).

The main objective of the present work is the calculation of WET and WER parameters considering several different tissue equivalent materials relevant in proton therapy. Some of those materials like bone, adipose and lung tissues were not considered in previous works. For this purpose, longitudinal dose distributions have been calculated using two Monte Carlo codes: TOPAS (Perl et al., 2012) and MCNP6.1 (Goorley et al., 2012). Differences on the results provided by these codes were analyzed and quantified using the stopping power database from the National Institute of Standards and Technology (NIST) for several proton energies in the therapeutic range from 70 to 225 MeV. Also, comparison of results obtained with different stopping power database has been analyzed to quantify its influence in the WER and WET determination.

2. Material and methods

2.1. Tissue-equivalent materials

According to report 44 of the International Commission for Radiation Units and Measurements (ICRU) (White, D. R., Booz, J., Griffith, R. V., Spokas, J. J., & Wilson, 1989), tissue equivalent materials can reproduce the radiation behavior of the reference material in a phantom, in order to evaluate the dose distribution (White, D. R., Booz, J., Griffith, R. V., Spokas, J. J., & Wilson, 1989). In the present work, 12 different tissue equivalent materials have been considered to estimate the water equivalence thickness. Table 1 shows the composition and density of each material used where natural isotopic concentration has been considered.

2.2. WET and WER calculations

In clinical practice, the WER parameter is considered due to the applications of water equivalence of the material in radiation dosimetry (Akbari, M., & Karimian, 2020; de Vera et al., 2014; Safigholi and Song, 2018). The WER is characterized as the ratio of the range (d_{80}) in water and in a phantom material (Bagheri et al., 2019), being defined by eq. (1):

$$WER = \frac{d_{80}^{water}}{d_{80}^{material}} \tag{1}$$

where d_{80} represents the range obtained through the longitudinal dose distribution curve corresponding to the depth where the dose assumes 80% of the maximum dose. It is measured in the distal part of the curve (Bagheri et al., 2019; Paganetti, 2012; Yoriyaz et al., 2019).

The presence of heterogeneities produces changes in the dose distribution, depending on the thickness, composition and density of the materials (Faiz and John, 2014). Knowing the thickness of the material through the WET calculation, it is possible to obtain the thickness of water, which causes a beam of protons to lose the same amount of energy, in which it would lose in the material (Akbari et al., 2014; Zhang and Newhauser, 2009). Fig. 1 shows the concept of WER and WET.

According to the study by Zhang and Newhauser (2009), an analytical way to calculate WET values was developed and it can be defined by eq. (2) (Zhang et al., 2010; Zhang and Newhauser, 2009):

$$WET = t_m \frac{\rho_m}{\rho_w} \frac{S_m}{S_w} \tag{2}$$

where ρ_w and S_w are the density and the mean proton mass stopping power of water; t_m, ρ_m and S_m are, respectively, the thickness, density, and the mean proton mass stopping power of the material. The mean proton mass stopping power can be defined by eq. (3) (Zhang and Newhauser, 2009):

$$\overline{S} = \frac{\int SdE}{\int dE} \tag{3}$$

In the present work the calculation of WET was based on the formulation proposed by Safigholi and Song (2018) where a material of thickness, t_m, is added to water, so that, the WET can be obtained through the difference between the range in water and that obtained in the presence of another material of interest, defined as eq. (4):

$$WET = d_{80}^{water} - d_{80}^{material-water} \tag{4}$$

Table 1
Density and composition of the 12 tissue equivalent materials used in this work. Compositions are in fraction by weight, except for polyethylene, polysthylene and water, which are in number of atoms.

Fraction by Weight												
Material	Density g/cm^3	Element and Atomic Number										
		H 1	C 6	N 7	O 8	Na 11	Mg 12	P 15	S 16	Cl 17	K 19	Ca 20
Adipose Tissue - ICRP	0.95	0.114	0.598	0.007	0.278	0.001	–	–	0.001	0.001	–	–
Brain - ICRP	1.04	0.107	0.145	0.022	0.712	0.002	–	0.004	0.002	0.003	0.003	–
Compact Bone - ICRU	1.85	0.064	0.278	0.027	0.410	–	0.002	0.070	0.002	–	–	0.147
Cortical Bone - ICRP	1.92	0.034	0.155	0.042	0.435	0.001	0.002	0.103	0.003	–	–	0.225
Eye Lens - ICRP	1.07	0.096	0.195	0.057	0.646	0.001	–	0.001	0.003	0.001	–	–
Lung - ICRP	1.04	0.105	0.083	0.023	0.779	0.002	–	0.001	0.002	0.003	0.002	–
Muscle Skeletal - ICRP	1.05	0.102	0.143	0.034	0.710	0.001	–	0.002	0.003	0.001	0.004	–
PMMA - Lucite	1.19	0.081	0.599	–	0.319	–	–	–	–	–	–	–
Polyethylene	0.94	2.000	1.000	–	–	–	–	–	–	–	–	–
Polystyrene	1.06	8.000	8.000	–	–	–	–	–	–	–	–	–
Soft Tissue - ICRP	1.03	0.105	0.256	0.027	0.602	0.001	–	0.002	0.003	0.002	0.002	–
Soft Tissue - ICRU-4	1.00	0.101	0.111	0.026	0.762	–	–	–	–	–	–	–
Water	1.00	2.000	–	–	1.000	–	–	–	–	–	–	–

ICRP - International Commission on Radiological Protection.

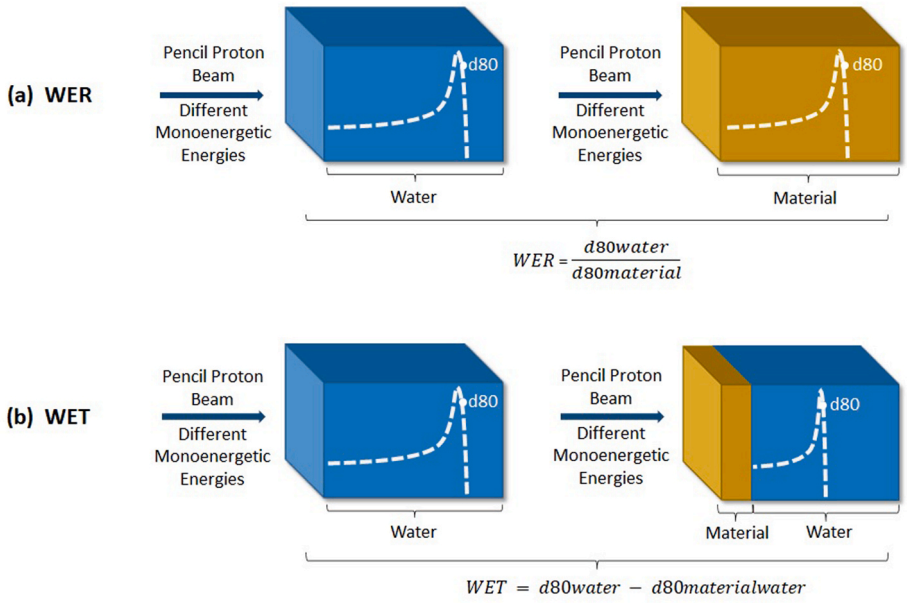

Fig. 1. Schematic representation for (a) WER and (b) WET calculations.

where, the term $d_{80}^{material-water}$ is the range of protons obtained with the presence of material m with thickness t_m added to the water phantom as shown in Fig. 1b. Four thickness values have been considered in the simulations: 0.5, 1.0, 1.5 and 2.0 cm. For the WER values, we considered the simulation setup shown in Fig. 1a and using eq. (1).

2.3. Simulations

The geometry of the phantom for simulation consisted of a box of tissue equivalent material with dimensions of 20 × 20 × 40 cm^3. Depth dose distribution was calculated in a grid of 4000 points (each step with 0.01 cm) placed in Z direction. The phantom was filled completely with water or tissue equivalent material which are: Adipose tissue – ICRP, Brain – ICRP, Compact Bone – ICRU, Cortical Bone – ICRP, Eye Lens – ICRP, Lung – ICRP, Muscle Skeletal – ICRP, PMMA – Lucite, Polyethylene, Polystyrene, Soft Tissue – ICRP and Soft Tissue – ICRU-4. Fig. 2 shows the geometry used in the simulations.

The radiation source consists of a monoenergetic proton beam with a circular shape with a radius of 0.2 cm positioned 5.0 cm distant from the phantom and in a vacuum media. The proton source energies were 70 MeV, 100 MeV, 125 MeV, 150 MeV, 175 MeV, 200 MeV and 225 MeV (Bagheri et al., 2019; Schuemann et al., 2014).

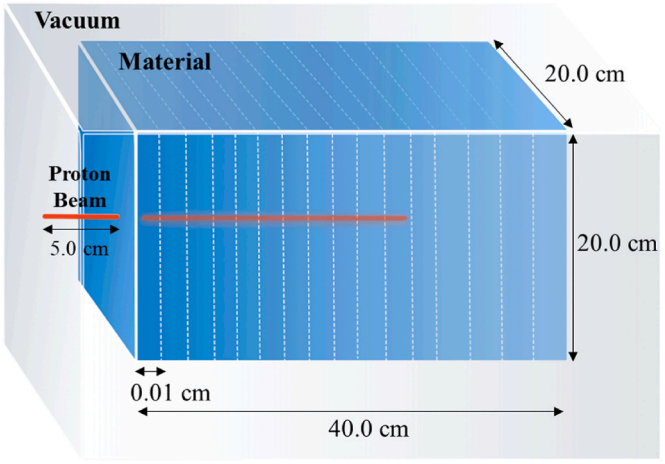

Fig. 2. Schematic representation of the geometry used for simulations with codes MCNP and TOPAS.

2.4. MCNP6.1 code

MCNP6 version 6.1 (J.T. Goorley et al., 2013) is able to transport several particles types including heavy ions. Physics models in the code are separated in basically 3 energy ranges: a) below 1.31 MeV the medium is treated as a gas of free electrons; b) above 5.24 MeV the stopping power is calculated from Bethe formula and; c) in the intermediate range of 1.31–5.24 MeV, the stopping power values are interpolated from previous range data (Zieb et al., 2018).

Depth dose distribution was obtained superimposing a grid of 4000 points over the geometry to obtain the fluence distribution (FMESH mesh tally) multiplied by the stopping powers data entered through DE/DF cards. This procedure allowed us a very high spatial resolution (0.01 cm) for interpolation of values in a very steep curve region near the Bragg Peak and consequently to be able to determine d_{80} with high precision.

2.5. TOPAS code

TOPAS is a user-friendly, multipurpose program that was initially created for medical physics application. TOPAS, current version 3.7.0, wraps around and extends the functionality of GEANT4 (version 10.06. p03), and in the present work, simulations were made using the default physics list suitable for proton therapy. This physics list has models that take into account the transport of protons and secondary particles although only protons were scored, as was the case in the MCNP simulations.

The physics models used in the simulations are listed in Table 2. In "G4EmStandardPhysics_option4", ionization is handled by several models depending on the particle type and energies for protons. The Bragg model is used for energies below 2 MeV and the Bethe-Bloch for higher energies. The geometry of the simulations followed exactly that previously defined by the MCNP6.1 for the parameters WET and WER, as well as, the spatial grid resolution of the scoring region.

2.6. Stopping powers on WET and WER calculations

To verify the influence of different stopping power data on WET and

Table 2
TOPAS default physics list used in simulations for dose calculation.

Modules	Simulated Interactions
g4em-standard_opt4	Electromagnetic physics. It's a combination of the most accurate EM models
g4h-phy_QGSP_BIC_HP	Nuclear interactions using Binary Intranuclear Cascade (BIC) Model. High Precision (HP) libraries are used to model the neutron elastic scattering for energies below 20 MeV.
g4decay	Decay of all long-lived nuclei.
g4ion-binarycascade	Nuclear interactions using binary cascade for light ions.
g4h-elastic_HP	Elastic scattering of hadrons. Uses High Precision libraries for neutrons with energies below 20 MeV.
g4stopping	Captures resting charged particles.

WER values, simulations were performed using the stopping power provided by NIST and from those calculated in TOPAS (Perl et al., 2012) and MCNP6 (Armstrong and Chandler, 1973; Bethe and Ashkin, 1953; Bichsel, 1972; Janni, 1982; Lindhard, 1954). For each material and energy, the beam range, d_{80}, was determined using an in-house script written in Python code version 3.8. In the script, a Gaussian curve was fitted between the longitudinal points of maximum dose and at 20% of the maximum dose in order to obtain the value of d_{80}.

2.7. Statistical analysis

In all simulations, the maximum statistical uncertainty was less than 1.0%. To achieve this precision the total number of proton histories simulated were 5×10^6 and 1×10^6, respectively, in MCNP6 and TOPAS. As the percentage differences, PD (%), between the MCNP6 (M) and TOPAS (T) results, were obtained using the TOPAS results as a reference, according to eq. (5).

$$PD(\%) = 100 * \frac{M - T}{T} \tag{5}$$

The proton energy cut-off value, Ecut, is the minimum energy for transport. This value was 100 eV for Topas and 1 keV for MCNP6. We have assured that the correspondent proton range for these energies are smaller than the smallest geometry dimension in the problem so that any proton with energy smaller than Ecut is locally absorbed.

3. Results and discussion

Fig. 3 shows the dependence of CSDA range from NIST with proton energy and the relative differences in percentage that exist when comparing stopping powers from different data (NIST, MCNP and TOPAS) for four different tissues: Adipose, Cortical Bone, Muscle Skeletal and Water. The most significant differences are found for cortical bone with a maximum difference of 1.60% and 1.90% at 70 MeV, respectively for two cases: a) the difference corresponds to the case when the stopping power data from NIST is compared to those extracted from the MCNP6 code; and b) the difference corresponds to the case when the stopping power data from NIST is compared to those extracted from TOPAS code. In general, however, in the therapeutic range (70–225 MeV), the agreement is very good among data for all tissue-equivalent material.

Dose profiles were simulated and the range was obtained for water and various materials, being used as an equivalence estimator. Table 3 shows the range d_{80} (cm) obtained with TOPAS and MCNP6 codes. The last one was used for simulation using different stopping power data for each material. The first one was assumed as a reference for computing the relative differences between values.

The maximum simulation statistical uncertainties in MCNP6 and TOPAS results were respectively 0.6% and 0.5%. From these results, in

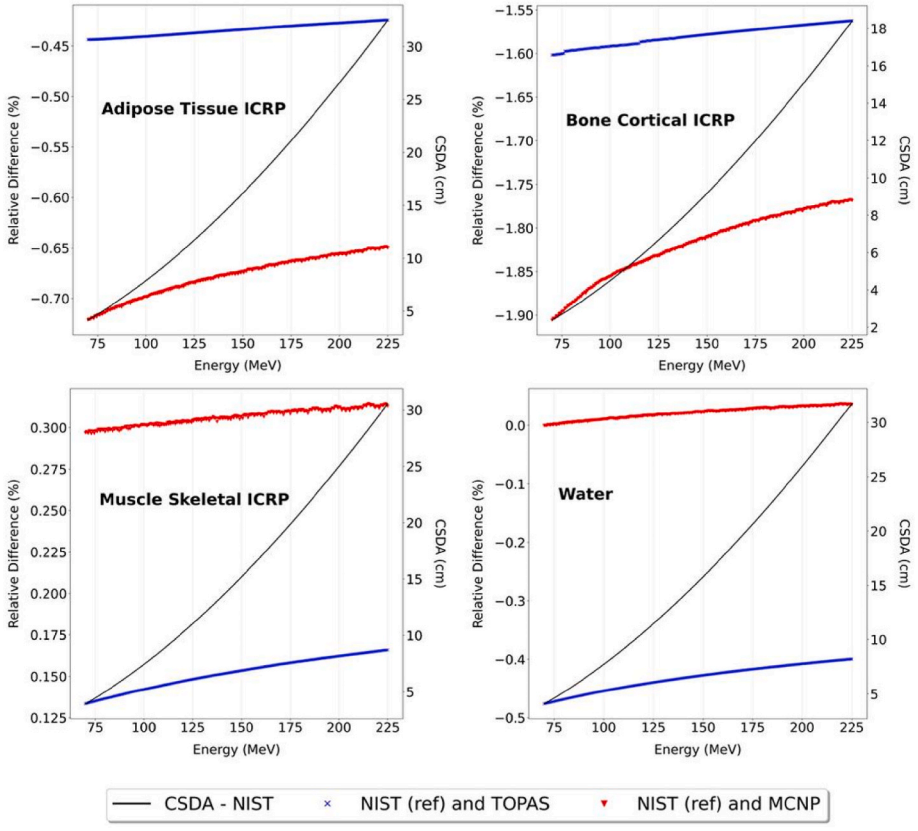

Fig. 3. The dependence of CSDA range from NIST with proton energy and relative differences of stopping powers obtained from different data (NIST, MCNP and TOPAS) for 4 different tissue-equivalent materials.

Table 3
Proton range (d_{80}) in cm for different tissue-equivalent materials and energies among results using different stopping power data.

Tissue-Equivalent Materials													
Energy MeV		**AD**	**B**	**CpB**	**CtB**	**EL**	**Lg**	**MS**	**PMMA**	**Pe**	**Py**	**StR**	**StU**	**W**
70	**Topas**	**4.18**	**3.92**	**2.37**	**2.42**	**3.84**	**3.94**	**3.92**	**3.51**	**4.06**	**3.92**	**3.95**	**4.11**	**4.10**
	N	4.20	–	2.37	2.42	–	–	3.92	3.50	4.06	3.90	–	–	4.08
	M	4.20	3.94	2.37	2.42	3.87	3.95	3.92	3.50	4.06	3.90	3.97	4.12	4.09
	T	4.20	3.94	2.37	2.42	3.87	3.95	3.92	3.50	4.06	3.90	3.97	4.12	4.08
100	**Topas**	**7.91**	**7.41**	**4.49**	**4.56**	**7.28**	**7.45**	**7.41**	**6.64**	**7.70**	**7.41**	**7.48**	**7.77**	**7.75**
	N	7.90	–	4.48	4.57	–	–	7.37	6.59	7.64	7.34	–	–	7.67
	M	7.90	7.40	4.48	4.58	7.27	7.43	7.37	6.59	7.64	7.34	7.46	7.75	7.67
	T	7.90	7.39	4.48	4.57	7.26	7.43	7.37	6.59	7.64	7.34	7.45	7.74	7.67
125	**Topas**	**11.76**	**11.02**	**6.66**	**6.77**	**10.81**	**11.07**	**11.01**	**9.86**	**11.44**	**11.02**	**11.12**	**11.54**	**11.50**
	N	11.78	–	6.64	6.79	–	–	10.97	9.80	11.39	10.93	–	–	11.43
	M	11.78	11.02	6.64	6.79	10.82	11.06	10.98	9.80	11.39	10.93	11.11	11.54	11.44
	T	11.78	11.02	6.64	6.79	10.82	11.06	10.97	9.80	11.39	10.93	11.10	11.54	11.43
150	**Topas**	**16.20**	**15.17**	**9.16**	**9.31**	**14.88**	**15.24**	**15.15**	**13.58**	**15.77**	**15.17**	**15.31**	**15.89**	**15.83**
	N	16.24	–	9.14	9.34	–	–	15.12	13.50	15.71	15.07	–	–	15.75
	M	16.24	15.18	9.14	9.34	14.91	15.25	15.13	13.51	15.71	15.07	15.31	15.91	15.76
	T	16.24	15.18	9.14	9.34	14.91	15.24	15.12	13.51	15.71	15.07	15.31	15.90	15.75
175	**Topas**	**21.19**	**19.83**	**11.97**	**12.15**	**19.46**	**19.93**	**19.81**	**17.76**	**20.62**	**19.83**	**20.02**	**20.78**	**20.69**
	N	21.21	–	11.95	12.19	–	–	19.76	17.66	20.54	19.70	–	–	20.58
	M	21.22	19.84	11.95	12.19	19.49	19.92	19.77	17.66	20.54	19.70	20.01	20.78	20.59
	T	21.21	19.84	11.95	12.19	19.48	19.92	19.76	17.66	20.54	19.70	20.00	20.78	20.58
200	**Topas**	**26.67**	**24.96**	**15.06**	**15.28**	**24.49**	**25.08**	**24.93**	**22.35**	**25.96**	**24.96**	**25.20**	**26.15**	**26.04**
	N	26.65	–	15.04	15.34	–	–	24.83	22.20	25.81	24.75	–	–	25.86
	M	26.66	24.93	15.05	15.34	24.49	25.03	24.84	22.21	25.82	24.76	25.14	26.10	25.87
	T	26.65	24.93	15.04	15.34	24.48	25.03	24.83	22.21	25.81	24.75	25.13	26.10	25.86
225	**Topas**	**32.62**	**30.52**	**18.40**	**18.68**	**29.95**	**30.67**	**30.48**	**27.34**	**31.75**	**30.53**	**30.81**	**31.98**	**31.84**
	N	32.55	–	18.39	18.73	–	–	30.31	27.11	31.53	30.22	–	–	31.57
	M	32.56	30.44	18.39	18.74	29.89	30.56	30.32	27.11	31.54	30.23	30.69	31.87	31.57
	T	32.55	30.43	18.39	18.73	29.89	30.55	30.31	27.11	31.53	30.22	30.68	31.86	31.57

AD – Adipose Tissue B – Brain – ICRP CpB – Compact Bone – ICRU.
CtB – Cortical Bone – ICRP EL – Eye Lens – ICRP Lg – Lung – ICRP.
MS – Muscle Skeletal – ICRP PMMA – Lucite Py – Polysthylene.
Pe – Polyethilene StR – Soft Tissue – ICRP StU – Soft Tissue – ICRU-4 W – Water.
Topas - Topas Values.
N – Percentage Difference (Topas versus MCNP6 w/NIST Stopping Power).
M – Percentage Difference (Topas versus MCNP6).
T – Percentage Difference (Topas versus MCNP6 w/Topas Stopping Power).

the therapeutic energy range, no significant differences in dose were observed when using different stopping power data presenting a maximum relative difference of around 1.0%. Also, the results obtained here have shown no differences comparing to those provided by Bagheri et al. (2019) for water, polysthylene, polyethylene and PMMA with a maximum discrepancy less than 0.5%.

Using eq. (1) and data from Table 3, WER values were obtained with TOPAS code in function of energy and shown in Fig. 3 for different tissue equivalent materials. The calculations were performed following the scheme presented in Fig. 1a. It can be observed that the values are almost independent of energy. The minimum (0.98) and maximum (1.73) WER values were, respectively, for adipose tissue and compact bone. The independence of WER with energy facilitates dose calculation process since the amount of water to substitute the tissue depends only of the amount of tissue and not of beam energy.

Soft tissue – ICRU presented the closest depth dose values to water followed by Polyethylene (PE) as mentioned by Bagheri et al. (2019) and can be observed in Fig. 4.

Comparison of all simulated WER values with those obtained with MCNP6 code are shown in Fig. 5 for each energy considered and using different stopping power data (SP MCNP6 – stopping power from MCNP6; SP NIST – stopping power from NIST and SP TOPAS – stopping power from TOPAS).

In general, the codes maintained good agreement, having relative differences less than 1.2% for the entire energy range. Materials with higher densities have higher WER values with respect to water. The highest range is found for Adipose Tissue (AD) and the lowest range for Compact Bone (CpB).

Table 4 shows the d_{80} with the presence of tissue-equivalent materials of different thickness and for all the energies considered in this study obtained with TOPAS code. From these values and using eq. (4) the WET values have been calculated and presented in Table 5.

Fig. 6 shows these values in function of material thickness for all materials and for the energies of 70 and 225 MeV demonstrating the linearity of WET with material thickness. Also, when comparing WET values of different materials one can observe that the smallest differences occur for lowest material thickness increasing as the thickness increases. It was also noted that these differences are almost constant for all energies as can be seen comparing the curves for both energies, 70 and 225 MeV.

Table 6 shows the linear coefficients obtained through the fit of the WET data for all energies according to eq. (6):

$$\mathrm{WET\ (cm)} = \mathrm{a.t_m} + \mathrm{b} \tag{6}$$

The values in parentheses in Table 6 show the uncertainties of the coefficients **a** and **b** in percentage, being less than 0.3%. Fit errors for all materials were less than 0.1%.

Previous study shown that, basically, two material components have influence in WET determination: material composition and density. Further analysis has shown that the composition has minor influence in contrast to density which has greatly influence in WET variation (Branco et al., 2019).

4. Conclusion

In general, very good agreement has been found between the range

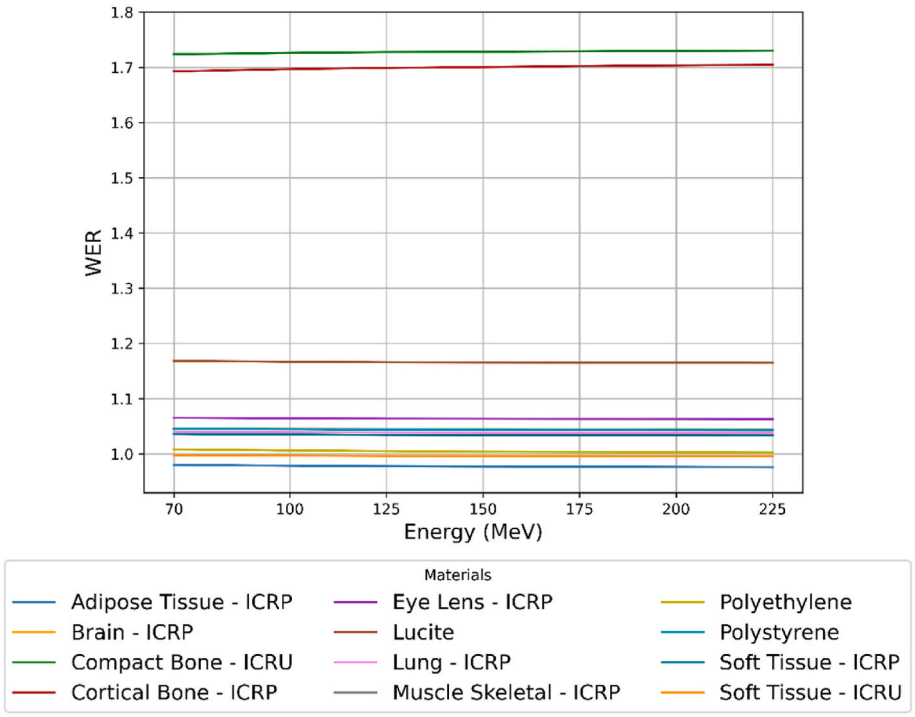

Fig. 4. WER values obtained with TOPAS for different materials and energies.

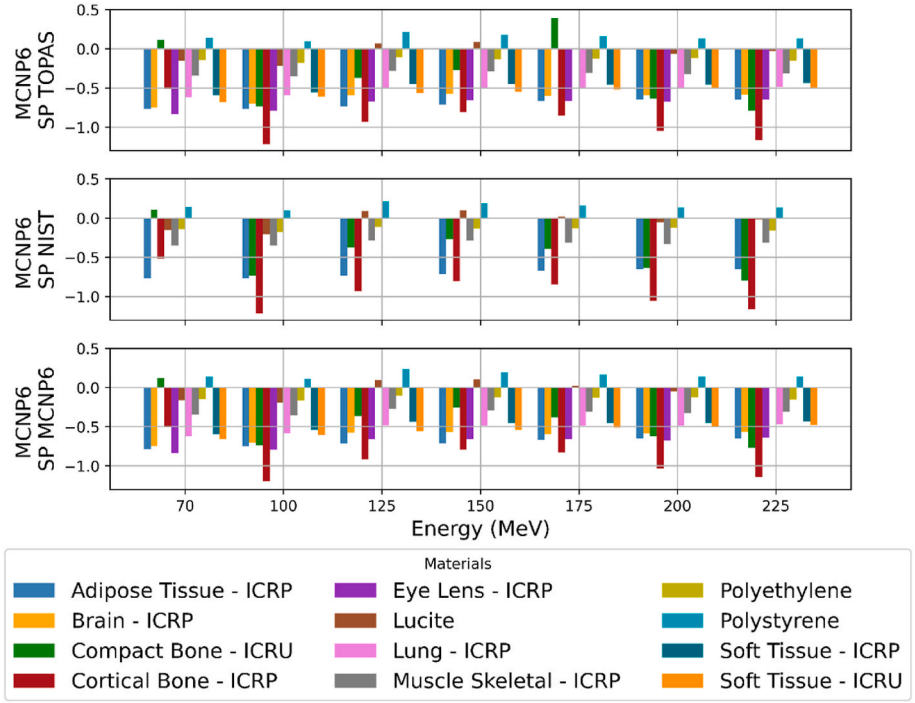

Fig. 5. Percentage differences (%) in WER between values obtained with TOPAS and MCNP6 codes using different Stopping Power (SP) data: SP MCNP6 – Stopping power from MCNP6; SP NIST – stopping power from NIST; SP TOPAS – stopping power from TOPAS.

and WET values obtained with two codes, and also, with those found in the literature for materials such as water, polysthylene, polyethylene and PMMA with a maximum difference less than 0.5%. Small differences were found when using different stopping power data for different tissue-equivalent materials (maximum of 1.9% for cortical bone at 70 MeV), but it did not affect the calculation of dose in the therapeutic range of energy of 70–225 MeV. We also demonstrate the linearity of WET with material thickness regardless of proton source energy considered. This aspect greatly simplifies the treatment planning procedure since the WET dependence on material thickness can be represented by a first-order polynomial. The highest range, d_{80}, was found for Adipose Tissue (AD) and the lowest range for Compact Bone (CpB) among all materials studied. The authors believe that the results presented in this work can provide important information for treatment

Table 4
Proton range d_{80} in cm for different tissue-equivalent materials with different thicknesses and energies.

Energy Mev	t_m (cm)	Tissue-equivalent Materials											
		AD	B	CpB	CtB	EL	Lg	MS	PMMA	Pe	Py	StR	StU
70	**0.5**	3.61	3.57	3.23	3.25	3.56	3.58	3.57	3.51	3.59	3.57	3.58	3.60
	1.0	3.12	3.05	2.37	2.48	3.03	3.06	3.05	2.93	3.09	3.05	3.06	3.10
	1.5	2.63	2.53	1.50	1.55	2.50	2.54	2.53	2.35	2.59	2.53	2.54	2.60
	2.0	2.14	2.01	0.64	0.70	1.97	2.02	2.00	1.76	2.08	2.01	2.03	2.10
100	**0.5**	7.26	7.22	6.88	6.89	7.21	7.23	7.22	7.16	7.24	7.22	7.23	7.25
	1.0	6.77	6.70	6.02	6.04	6.68	6.71	6.70	6.58	6.74	6.70	6.71	6.75
	1.5	6.28	6.18	5.15	5.19	6.15	6.19	6.18	6.00	6.24	6.18	6.19	6.25
	2.0	5.79	5.66	4.29	4.34	5.62	5.67	5.66	5.41	5.74	5.66	5.68	5.75
125	**0.5**	11.01	10.97	10.63	10.64	10.96	10.98	10.97	10.91	10.99	10.97	10.98	11.00
	1.0	10.52	10.45	9.76	9.79	10.43	10.46	10.45	10.33	10.49	10.45	10.46	10.50
	1.5	10.03	9.93	8.90	8.94	9.90	9.94	9.93	9.75	9.99	9.93	9.95	10.00
	2.0	9.54	9.41	8.03	8.09	9.37	9.42	9.41	9.17	9.49	9.41	9.43	9.50
150	**0.5**	15.34	15.30	14.96	14.97	15.29	15.30	15.30	15.24	15.32	15.30	15.31	15.33
	1.0	14.85	14.78	14.09	14.12	14.76	14.79	14.78	14.66	14.82	14.78	14.79	14.83
	1.5	14.36	14.26	13.23	13.27	14.23	14.27	14.26	14.08	14.32	14.26	14.28	14.33
	2.0	13.87	13.74	12.36	12.41	13.70	13.75	13.74	13.50	13.82	13.74	13.76	13.83
175	**0.5**	20.20	20.16	19.82	19.83	20.15	20.17	20.16	20.10	20.19	20.16	20.17	20.19
	1.0	19.71	19.64	18.95	18.98	19.62	19.65	19.64	19.52	19.68	19.64	19.65	19.69
	1.5	19.22	19.12	18.09	18.12	19.09	19.13	19.12	18.94	19.18	19.12	19.14	19.19
	2.0	18.73	18.60	17.22	17.27	18.56	18.61	18.60	18.36	18.68	18.60	18.62	18.70
200	**0.5**	25.55	25.51	25.16	25.18	25.50	25.51	25.51	25.50	25.53	25.51	25.52	25.53
	1.0	25.06	24.99	24.30	24.32	24.97	25.00	24.99	24.87	25.03	24.99	25.00	25.04
	1.5	24.57	24.47	23.44	23.47	24.44	24.48	24.47	24.29	24.53	24.47	24.48	24.54
	2.0	24.08	23.95	22.57	22.62	23.91	23.96	23.94	23.71	24.03	23.95	23.97	24.04
225	**0.5**	31.34	31.31	30.96	30.97	31.30	31.31	31.30	31.24	31.33	31.31	31.31	31.33
	1.0	30.86	30.79	30.10	30.12	30.77	30.79	30.78	30.66	30.83	30.79	30.80	30.84
	1.5	30.37	30.27	29.23	29.27	30.24	30.27	30.26	30.08	30.33	30.27	30.28	30.34
	2.0	29.88	29.74	28.36	28.41	29.71	29.76	29.74	29.50	29.83	29.74	29.76	29.84

Table 5
WET in cm for different materials, thicknesses and energies.

WET (cm)													
Energy Mev	t_m (cm)	Material											
		AD	**B**	**CpB**	**CtB**	**EL**	**Lg**	**MS**	**PMMA**	**Pe**	**Py**	**StR**	**StU**
70	**0.5**	0.49	0.53	0.87	0.86	0.54	0.52	0.53	0.59	0.51	0.53	0.52	0.50
	1.0	0.98	1.05	1.73	1.70	1.07	1.04	1.05	1.17	1.01	1.05	1.04	1.00
	1.5	1.47	1.57	2.60	2.55	1.60	1.56	1.57	1.76	1.51	1.57	1.56	1.50
	2.0	1.96	2.09	3.46	3.40	2.13	2.08	2.10	2.34	2.02	2.09	2.08	2.00
100	**0.5**	0.49	0.53	0.87	0.86	0.54	0.52	0.53	0.59	0.51	0.53	0.52	0.51
	1.0	0.98	1.05	1.73	1.71	1.07	1.04	1.05	1.17	1.01	1.05	1.04	1.00
	1.5	1.47	1.57	2.60	2.56	1.60	1.56	1.57	1.75	1.51	1.57	1.56	1.50
	2.0	1.96	2.09	3.46	3.41	2.13	2.08	2.10	2.34	2.01	2.09	2.07	2.00
125	**0.5**	0.50	0.53	0.88	0.86	0.54	0.53	0.53	0.59	0.51	0.53	0.53	0.51
	1.0	0.99	1.06	1.74	1.72	1.08	1.05	1.06	1.18	1.02	1.05	1.05	1.01
	1.5	1.48	1.58	2.61	2.57	1.61	1.57	1.58	1.76	1.51	1.58	1.56	1.50
	2.0	1.96	2.10	3.47	3.42	2.14	2.09	2.10	2.34	2.02	2.10	2.08	2.00
150	**0.5**	0.50	0.54	0.88	0.87	0.54	0.53	0.54	0.59	0.51	0.53	0.53	0.51
	1.0	0.99	1.06	1.75	1.72	1.08	1.05	1.06	1.18	1.02	1.05	1.05	1.01
	1.5	1.48	1.58	2.61	2.57	1.61	1.57	1.58	1.76	1.52	1.58	1.56	1.51
	2.0	1.96	2.10	3.47	3.42	2.14	2.09	2.10	2.34	2.01	2.10	2.08	2.00
175	**0.5**	0.50	0.54	0.88	0.87	0.55	0.53	0.54	0.60	0.51	0.54	0.53	0.51
	1.0	0.99	1.06	1.75	1.72	1.08	1.05	1.06	1.18	1.02	1.06	1.05	1.01
	1.5	1.48	1.58	2.61	2.58	1.61	1.57	1.58	1.76	1.52	1.58	1.56	1.51
	2.0	1.96	2.10	3.48	3.43	2.14	2.09	2.10	2.34	2.02	2.10	2.08	2.00
200	**0.5**	0.50	0.54	0.88	0.87	0.55	0.54	0.54	0.55	0.52	0.54	0.53	0.51
	1.0	0.99	1.06	1.75	1.73	1.08	1.05	1.06	1.18	1.02	1.06	1.05	1.01
	1.5	1.48	1.58	2.61	2.58	1.61	1.57	1.58	1.76	1.52	1.58	1.56	1.51
	2.0	1.96	2.10	3.48	3.43	2.14	2.09	2.10	2.34	2.02	2.10	2.08	2.01
225	**0.5**	0.50	0.54	0.88	0.87	0.55	0.53	0.54	0.60	0.52	0.54	0.53	0.51
	1.0	0.99	1.05	1.74	1.72	1.07	1.05	1.06	1.18	1.02	1.06	1.05	1.01
	1.5	1.47	1.57	2.61	2.57	1.60	1.57	1.58	1.76	1.52	1.58	1.57	1.51
	2.0	1.96	2.10	3.48	3.43	2.14	2.09	2.10	2.34	2.02	2.10	2.08	2.01

planning to predict dose in human body tissues in proton therapy.

Author statement

Ana Laura Burin: Methodology, Software, Validation, Formal analysis, Data Curation, Writing - Original Draft, Visualization, Funding acquisition **Isabela Soares Lopes Branco:** Methodology, Software, Validation, Data Curation, Writing - Original Draft, Visualization, Funding acquisition. **Hélio Yoriyaz**: Conceptualization, Validation, Resources, Writing - Original Draft, Writing - Review & Editing,

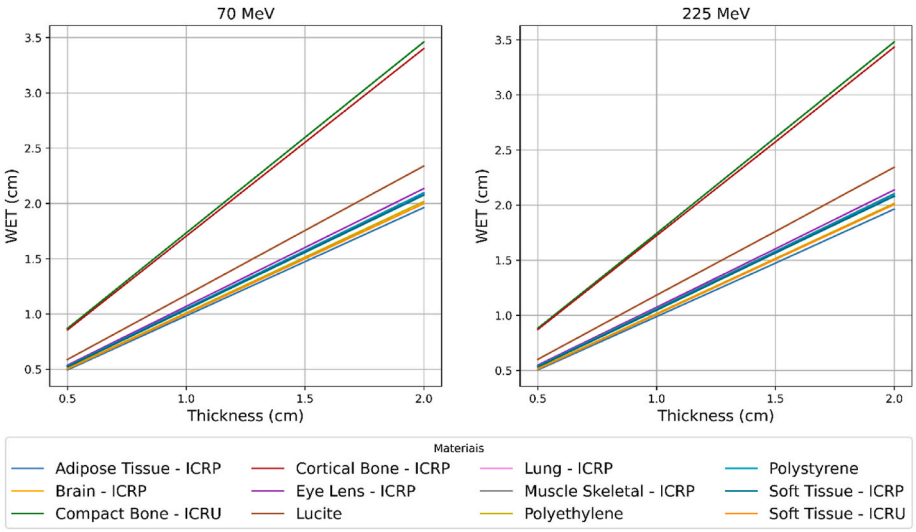

Fig. 6. WET (cm) in function of material thickness for different materials for the energies of 70 and 225 MeV.

Table 6
WET Linear coefficients for each material (In parentheses are the uncertainties of the coefficients a and b in percentage).

Materials	WET = a.t_m + b	
	a	b
Adipose Tissue - ICRP	0.9758 (0.07)	0.0106 (0.09)
Brain - ICRP	1.0426 (0.05)	0.0113 (0.06)
Compact Bone - ICRU	1.7301 (0.02)	0.0117 (0.02)
Cortical Bone - ICRP	1.7038 (0.04)	0.0122 (0.05)
Eye Lens - ICRP	1.0619 (0.02)	0.0118 (0.02)
Lucite - PMMA	1.1679 (0.2)	0.0050 (0.3)
Lung - ICRP	1.0379 (0.2)	0.0104 (0.2)
Muscle Skeletal - ICRP	1.0441 (0.05)	0.0116 (0.07)
Polyethylene	1.0012 (0.04)	0.0125 (0.05)
Polystyrene	1.0420 (0.02)	0.0118 (0.02)
Soft Tissue - ICRP	1.0326 (0.01)	0.0117 (0.02)
Soft Tissue - ICRU	0.9947 (0.07)	0.0115 (0.1)

Supervision, Project administration.

Declaration of competing interest

The authors declare the following financial interests/personal relationships which may be considered as potential competing interests: Ana Laura Burin reports financial support was provided by Coordination of Higher Education Personnel Improvement. Isabela Soares Lopes Branco reports financial support was provided by National Council for Scientific and Technological Development.

Data availability

Data will be made available on request.

Acknowledgments

Ana Laura Burin reports financial support was provided by Coordination of Higher Education Personnel Improvement. Isabela Soares Lopes Branco reports financial support was provided by National Council for Scientific and Technological Development.

References

Agostinelli, S., Allison, J., Amako, K., Apostolakis, J., Araujo, H., Arce, P., Asai, M., Axen, D., Banerjee, S., Barrand, G., Behner, F., Bellagamba, L., Boudreau, J., Broglia, L., Brunengo, A., Burkhardt, H., Chauvie, S., Chuma, J., Chytracek, R., Cooperman, G., Cosmo, G., Degtyarenko, P., Dell'Acqua, A., Depaola, G., Dietrich, D., Enami, R., Feliciello, A., Ferguson, C., Fesefeldt, H., Folger, G., Foppiano, F., Forti, A., Garelli, S., Giani, S., Giannitrapani, R., Gibin, D., Gomez Cadenas, J.J., Gonzalez, I., Gracia Abril, G., Greeniaus, G., Greiner, W., Grichine, V., Grossheim, A., Guatelli, S., Gumplinger, P., Hamatsu, R., Hashimoto, K., Hasui, H., Heikkinen, A., Howard, A., Ivanchenko, V., Johnson, A., Jones, F.W., Kallenbach, J., Kanaya, N., Kawabata, M., Kawabata, Y., Kawaguti, M., Kelner, S., Kent, P., Kimura, A., Kodama, T., Kokoulin, R., Kossov, M., Kurashige, H., Lamanna, E., Lampen, T., Lara, V., Lefebure, V., Lei, F., Liendl, M., Lockman, W., Longo, F., Magni, S., Maire, M., Medernach, E., Minamimoto, K., Mora de Freitas, P., Morita, Y., Murakami, K., Nagamatu, M., Nartallo, R., Nieminen, P., Nishimura, T., Ohtsubo, K., Okamura, M., O'Neale, S., Oohata, Y., Paech, K., Perl, J., Pfeiffer, A., Pia, M.G., Ranjard, F., Rybin, A., Sadilov, S., di Salvo, E., Santin, G., Sasaki, T., Savvas, N., Sawada, Y., Scherer, S., Sei, S., Sirotenko, V., Smith, D., Starkov, N., Stoecker, H., Sulkimo, J., Takahata, M., Tanaka, S., Tcherniaev, E., Safai Tehrani, E., Tropeano, M., Truscott, P., Uno, H., Urban, L., Urban, P., Verderi, M., Walkden, A., Wander, W., Weber, H., Wellisch, J.P., Wenaus, T., Williams, D.C., Wright, D., Yamada, T., Yoshida, H., Zschiesche, D., 2003. GEANT4 - a simulation toolkit. Nucl. Instruments Methods Phys. Res. Sect. A Accel. Spectrometers, Detect. Assoc. Equip. 506, 250–303. https://doi.org/10.1016/S0168-9002(03)01368-8.

Akbari, M., Karimian, A., 2020. Impact of transverse magnetic fields on water equivalent ratios in carbon-ion radiotherapy. J. Instrum. 15 https://doi.org/10.1088/1748-0221/15/05/t05006.

Akbari, M.R., Yousefnia, H., Mirrezaei, E., 2014. Calculation of water equivalent ratio of several dosimetric materials in proton therapy using FLUKA code and SRIM program. Appl. Radiat. Isot. 90, 89–93. https://doi.org/10.1016/j.apradiso.2014.03.012.

Armstrong, T.W., Chandler, K.C., 1973. Stopping powers and ranges for muons, charged pions, protons, and heavy ions. Nucl. Instrum. Methods 113, 313–314. https://doi.org/10.1016/0029-554X(73)90852-5.

Bagheri, R., Khorrami Moghaddam, A., Azadbakht, B., Akbari, M.R., Shirmardi, S.P., 2019. Determination of water equivalent ratio for some dosimetric materials in proton therapy using MNCPX simulation tool. Nucl. Sci. Tech. 30, 1–10. https://doi.org/10.1007/s41365-019-0544-z.

Bethe, H.A., Ashkin, J., 1953. Passage of radiations through matter. Exp. Nucl. Phys 166–252.

Bichsel, H., 1972. Passage of Charged Particles through Matter, third ed. Inst. Phys. Handb.

Branco, I.S.L., Antunes, P.C.G., Siqueira, P. de T.D., Shorto, J.M.B., Yoriyaz, H., 2019. Estudo dos Efeitos de Composição e Densidade de Materiais Tecido Equivalentes na Distribuição de Dose Longitudinal em Protonterapia. Rev. Bras. Física Médica 13, 2. https://doi.org/10.29384/rbfm.2019.v13.n3.p2-7.

de Vera, P., Abril, I., Garcia-Molina, R., 2014. Water equivalent properties of materials commonly used in proton dosimetry. Appl. Radiat. Isot. 83, 122–127. https://doi.org/10.1016/j.apradiso.2013.01.023.

Faiz, M.K., John, P.G., 2014. The Physics of Radiation Therapy, fifth ed.

Ferrari, A., Sala, P.R., Fasso, A., Ranft, J., 2005. FLUKA: a multi-particle transport code. Eur. Organ. Nucl. Res. Cern.

Goorley, T., James, M., Booth, T., Brown, F., Bull, J., Cox, L.J., Durkee, J., Elson, J., Fensin, M., Forster, R.A., Hendricks, J., Hughes, H.G., Johns, R., Kiedrowski, B., Martz, R., Mashnik, S., McKinney, G., Pelowitz, D., Prael, R., Sweezy, J., Waters, L., Wilcox, T., Zukaitis, T., 2012. Initial MCNP6 release overview. Nucl. Technol. 180, 298–315. https://doi.org/10.13182/NT11-135.

Goorley, J.T., James, M.R., Booth, T.E., Brown, F.B., Bull, J.S., Cox, L.J., J, W.D., Elson, J. S., Fensin, M.L., Forster, R.A., Hendricks, J.S., Hughes, H.G., Johns, R.C., B, C., Kiedrowski, S.G.M., 2013. MCNP6 User's Manual. LA-CP-13-00634. LANL Version 1., p. 765

Janni, J.F., 1982. Energy loss, range, path length, time-of-flight, straggling, multiple scattering, and nuclear interaction probability. In two parts. Part 1. For 63 compounds Part 2. For elements $1 \leq Z \leq 92$. At. Data Nucl. Data Tables 27, 147–339. https://doi.org/10.1016/0092-640X(82)90004-3.

Lindhard, J., 1954. On the properties of a gas of charged particles. Danske Mat. Meddelelser.

Lourenço, A., Shipley, D., Wellock, N., Thomas, R., Bouchard, H., Kacperek, A., Fracchiolla, F., Lorentini, S., Schwarz, M., Macdougall, N., Royle, G., Palmans, H., 2017. Evaluation of the water-equivalence of plastic materials in low- and high-energy clinical proton beams. Phys. Med. Biol. 3883–3901. https://doi.org/10.1088/1361-6560/aa67d4.

Matney, J.E., Park, P.C., Li, H., Court, L.E., Zhu, X.R., Dong, L., Liu, W., Mohan, R., 2016. Perturbation of water-equivalent thickness as a surrogate for respiratory motion in proton therapy. J. Appl. Clin. Med. Phys. 17, 368–378. https://doi.org/10.1120/jacmp.v17i2.5795.

Paganetti, H., 2012. Range uncertainties in proton therapy and the role of Monte Carlo simulations. Phys. Med. Biol. 57 https://doi.org/10.1088/0031-9155/57/11/R99.

Perl, J., Shin, J., Schümann, J., Faddegon, B., Paganetti, H., 2012. TOPAS: an innovative proton Monte Carlo platform for research and clinical applications. Med. Phys. 39, 6818–6837. https://doi.org/10.1118/1.4758060.

Safigholi, H., Song, W.Y., 2018. Calculation of water equivalent ratios for various materials at proton energies ranging 10-500 MeV using MCNP, FLUKA, and GEANT4 Monte Carlo codes. Phys. Med. Biol. 63, 9. https://doi.org/10.1088/1361-6560/aad0bd.

Schuemann, J., Dowdell, S., Grassberger, C., Min, C.H., Paganetti, H., 2014. Site-specific range uncertainties caused by dose calculation algorithms for proton therapy. Phys. Med. Biol. 59, 4007–4031. https://doi.org/10.1088/0031-9155/59/15/4007.

Veiga, C., Janssens, G., Teng, C., Baudier, T., Hotoiu, L., Mcclelland, J.R., Royle, G., Lin, L., Yin, L., Metz, J., Solberg, T.D., Tochner, Z., Simone, C.B., Mcdonough, J., Teo, B.K., 2016. First clinical investigation of cone beam computed tomography and deformable registration for adaptive proton therapy for lung cancer. Radiat. Oncol. Biol. 95, 549–559. https://doi.org/10.1016/j.ijrobp.2016.01.055.

Wang, P., Yin, L., Zhang, Y., Kirk, M., Song, G., Ahn, P.H., Lin, A., Gee, J., Dolney, D., Solberg, T.D., Maughan, R., Mcdonough, J., Teo, B.K., 2016. Quantitative assessment of anatomical change using a virtual proton depth radiograph for adaptive head and neck proton therapy. J. Appl. Clin. Med. Phys. 17, 427–440. https://doi.org/10.1120/jacmp.v17i2.5819.

White, D.R., Booz, J., Griffith, R.V., Spokas, J.J., Wilson, I.J., 1989. Tissue Substitutes in Radiation Dosimetry and Measurement, vol. 44. ICRU report. https://doi.org/10.1093/jicru/os23.1.report44.

Yoriyaz, H., Branco, I.S., Almeida, I.P., Fonseca, G.P., 2019. Fundamentos de Transporte e Cálculo de Dose em Tratamentos com Feixes de Prótons. Rev. Bras. Física Médica 13, 109. https://doi.org/10.29384/rbfm.2019.v13.n1.p109-115.

Zhang, R., Newhauser, W.D., 2009. Calculation of water equivalent thickness of materials of arbitrary density, elemental composition and thickness in proton beam irradiation. Phys. Med. Biol. 54, 1383–1395. https://doi.org/10.1088/0031-9155/54/6/001.

Zhang, R., Taddei, P.J., Fitzek, M.M., Newhauser, W.D., 2010. Water equivalent thickness values of materials used in beams of protons, helium, carbon and iron ions. Phys. Med. Biol. 55, 2481–2493. https://doi.org/10.1088/0031-9155/55/9/004.

Zieb, K., Hughes, H.G., James, M.R., Xu, X.G., 2018. Review of heavy charged particle transport in MCNP6.2. Nucl. Instruments Methods Phys. Res. Sect. A Accel. Spectrometers, Detect. Assoc. Equip. 886, 77–87. https://doi.org/10.1016/j.nima.2018.01.002.

Ziegler, J.F., Biersack, J.P., Ziegler, M.D., 2008. SRIM -The Stopping and Range of Ions in Matter. Lulu Press, 1–2.